10th International Conference on Fracture Mechanics of Concrete and Concrete Structures
FraMCoS-X
G. Pijaudier-Cabot, P. Grassl and C. La Borderie (Eds)
https://doi.org/10.21012/FC10.235508

EFFECT OF THE SPATIAL CORRELATION OF DAMAGE PROPERTIES OF CONCRETE ON THE STRUCTURAL CRACKING PATTERNS

D. E.-M. BOUHJITI[*,†], J. BAROTH[*], M. BRIFFAUT[*] AND F. DUFOUR[*]

[*] Univ. Grenoble Alpes, CNRS, Grenoble INP[1], 3SR, F-38000 Grenoble, France
† EGIS Industries, 4 rue Dolores Ibarruri Montreuil, TSA 50012-93188, France
e-mail: david.bouhjiti@3sr-grenoble.fr, www.3sr-grenoble.fr

Key words: concrete, cracking, size effects, random fields, early age, containment buildings

Abstract: Concrete is inherently a heterogeneous and aging material. Its properties are spatially scattered and constantly evolving in time. This leads to a different behavior at each elementary volume of the structure. One way to simulate the effect of this randomness is to use discretized and FE-projected random fields according to a certain spatial correlation function and a property-dependent fluctuation length. In the particular case of concrete cracking simulation, and to account for the statistical size effects, those random fields are commonly associated with the damage strain threshold. However, their properties are rarely completely identified and remain, in most cases, arbitrary. In this paper, using a continuous local unilateral and energy-regularized damage model, the sensitivity analysis of the structural cracking response to such *a priori* hypotheses is studied. In particular, the effects of spatial correlation (none, Gaussian, linear, exponential, sinusoidal) on the resultant cracking patterns are explored. As an application, the experimental 1:3 scaled containment building named VeRCoRs is considered at the early age phase under quasi-homogenous tensile loads (where cracking is due to restrained thermal and endogenous shrinkages). The results show a strong dependency of the observed frequency of each cracking pattern to the numerically implemented spatial correlation of the damage strain threshold and softening law. This should encourage the measurement of, at least, the spatial scattering of the Young's modulus and the tensile strength defining the damage strain threshold; which would enhance the characterization of the implemented random fields and improve their use to simulate realistic cracking patterns and their associated frequencies of occurrence.

[1] Institute of Engineering Univ. Grenoble Alpes

1 INTRODUCTION

The initiation and propagation of cracks in concrete is driven by the spatial distributions of, both, the tensile stress field and the voids and defects in the volume defining its mechanical strength [1]. From a modeling point of view, the mathematical description of the cracking process needs to account for both aspects; usually referred to by ''size effects'' [2]. Usually, two types of size effects are addressed in the literature:

- Statistical size effect: from a conceptual point of view, it refers to the effects of material strength randomness in the volume (descriptive of the distribution of defects and voids) on its damage behavior. This induces two things (a) given the weakest link theory introduced by Weibull in [3], the size of defects is expected – statistically – to increase with the size of the considered volume leading to a reduction of its tensile strength and (b) the position of defects being random, the initiation point of cracks and its propagation paths are random as well.
- Energetic size effect: as the crack propagates, dissipative energy is released (fracture energy) within a so-called Fracture Process Zone (FPZ) ahead of the crack tip. The shape of the FPZ and its extent, in addition to an intrinsic material dependency, are strongly dependent on the stress state in concrete [3]. For concrete, being a quasi-brittle material, the fracture is preceded by a rather large FPZ of variable size which affects considerably the post-peak (softening) behavior of concrete [5].

Eventually, and based on the contribution of several authors to the issue of size effects, statistical and energetic size effects lead to the definition of a probabilistic-based, stress dependent and non-local Size Effect Law (SEL) in eq.1 [2][4][6-7] where the material strength at a given position $\overrightarrow{x_0}$ of the domain of interest Ω, represented by the tensile strength R_t, is dependent on a material-dependent constant D_c defining the extent of fracture energy dissipation and m the Weibull factor, on the tensile stress distribution over the FPZ $\boldsymbol{\sigma}_+(x)$ and on a weighing function Ψ representing the decreasing effect of elementary volumes at a position $\vec{x}$ as they become distant from the point of interest $\overrightarrow{x_0}$.

$$\frac{R_t(\overrightarrow{x_0}\in\Omega)}{R_{t,ref}(V_{ref})} = \left(\frac{\int_{\vec{x}\in\Omega}\Psi(|\vec{x}-\overrightarrow{x_0}|,\ D_c,\ \boldsymbol{\sigma}_+(x))\,d\vec{x}}{V_{ref}}\right)^{-\frac{1}{m}} \quad (1)$$

Nevertheless, one should note that eq. 1 does not allow a proper simulation of the spatial randomness of localization and propagation due to concrete's heterogeneity. To overcome such limitation, several authors explicitly model the spatial scattering of the tensile strength R_t [8] or the Young's modulus E [9] (defining the strain damage threshold $\varepsilon_{d0,t} = \frac{R_t}{E}$) using discretized, FE-projected Random Fields (RF) (case of normal distribution in eq. 2 [10]).

$$\begin{aligned} Z(\vec{x}\in\Omega) &= \mu_Z + \sum_{i=1}^{\infty}\sqrt{\lambda_i}\varphi_i(\vec{x})\,\xi_i \\ C_Z(\vec{x},\vec{y}\in\Omega) &= \sigma_Z^2\,\rho_Z\big([\vec{x}-\vec{y}],l_{flu,Z}\big) \\ l_{flu,Z} &= \int_{-\infty}^{+\infty}\rho_Z\big(|\vec{x}-\vec{y}|,l_{flu,Z}\big)\,d|\vec{x}-\vec{y}| \end{aligned} \quad (2)$$

for a given Z quantity, (μ_Z,σ_Z) are the mean and standard deviation, (λ_i,φ_i) are the Eigen values and vectors respectively of the covariance matrix C_Z, ρ_Z is the autocorrelation function and l_{flu} its associated fluctuation length defined in the sense of [11].

Indeed, the combination of the SEL and RF leads to a Statistical Size Effect Law (SSEL) descriptive of a volume-dependent and spatially variable behavior law for each elementary volume in the simulated domain which, conceptually, enhances the simulation of random cracks' initiation and propagation.

However, it seems that the use of RF is generally considered as, merely, a numerical artifact to facilitate strain localization and its effect on the cracking response is supposed negligible. This is seen through the use of arbitrary correlation functions (usually Gaussian ρ_Z [9][12]) or no correlation at all

[8]. Though the effect of RF correlation is expected to be less influential on the cracking response in the presence of strong stress gradients, such hypothesis cannot be generalized to all configurations; in particular in the presence of (quasi-)homogeneous tensile loads.

Hence, this contribution aims at answering the question related to the sensitivity of the cracking response to the spatial scattering of concrete cracking properties. This is achieved through three parts following the present introduction:

- The first part recalls the main hypothesis of the used damage model.
- The second part focuses on the implementation of the presented SSEL.
- The last part explores the effect of the spatial correlation on the cracking response at early age of a Representative Structural Volume (RSV) of a containment building at the 1:3 scale [13].

2 DAMAGE MODEL

For the purpose of the forthcoming application at early age, a staggered thermo-mechanical model is retained.

2.1 Thermo-mechanical model

The first step consists of solving the heat equation with a non-null source term (3) to define the field of temperature T and its evolution over time during the hydration phase. As the hydration kinetic becomes negligible ($\frac{d\alpha}{dt} \to 0$), temperature evolution is mainly driven by the variation of the thermal boundary conditions considered herein as convective mainly.

$$\frac{dT}{dt} - \frac{\lambda_c}{\rho_c C_c^p} \nabla^2 T = \frac{Q_\infty}{\rho_c C_c^p} \frac{d\alpha}{dt} e^{-\frac{E_a^{th}}{RT(t)}} \quad (3)$$

where ρ_c is the concrete's density, C_c^p the thermal capacity, λ_c is the thermal capacity, Q_∞ the hydration heat, α the hydration rate, E_a^{th} the activation energy and R the universal gas constant.

Then, a second calculation is undertaken aiming at the description of the mechanical behavior of concrete during the hydration phase. The total strain tensor $\boldsymbol{\varepsilon_{TOT}}$ is decomposed into four components (eq. 4): the elastic $\boldsymbol{\varepsilon_{ELAS}}$, the thermal $\boldsymbol{\varepsilon_{TH}}$, the endogenous $\boldsymbol{\varepsilon_{ES}}$ and the basic creep $\boldsymbol{\varepsilon_{BC}}$ ones.

$$\boldsymbol{\varepsilon_{TOT}} = \boldsymbol{\varepsilon_{ELAS}} + \boldsymbol{\varepsilon_{TH}} + \boldsymbol{\varepsilon_{ES}} + \boldsymbol{\varepsilon_{BC}} \quad (4)$$

The thermal and endogenous strain tensors are assumed isotropic and linearly related to the temperature and hydration rate evolutions in time respectively.

$$\begin{aligned} \boldsymbol{\varepsilon_{TH}} &= \alpha_{TH} (T - T_0) \mathbf{I_d} \\ \boldsymbol{\varepsilon_{ES}} &= -\alpha_{ES} (\alpha - \alpha_0) \mathbf{I_d} \end{aligned} \quad (5)$$

with α_{TH}, α_{ES} the thermal and endogenous shrinkage coefficients respectively, $\mathbf{I_d}$ the identity tensor.

And the basic creep strain tensor is computed according the Burgers rheological model accounting for the hydration effect, the thermo-activation and irreversibility aspects [9].

2.2 Damage model

As damage calculations at the structural scale require hefty computational time, a local damage model is retained herein rather than a nonlocal one; in particular a unilateral and isotropic formulation is considered [14].

$$\boldsymbol{\sigma} = (1 - d)\mathbf{C_0} : \boldsymbol{\varepsilon} \quad (6)$$

with d the scalar damage variable (varying between 0 and 1), $\mathbf{C_0}$ the elastic compliance tensor, $(\boldsymbol{\sigma}, \boldsymbol{\varepsilon})$ the stress and strain tensors respectively.

For the tensile part, the tensile damage variable writes [15]:

$$\begin{aligned} d &= < 1 - \frac{\varepsilon_{d0,t}}{Y_t} e^{-B_t (Y_t - \varepsilon_{d0,t})} >_+ \\ Y_t &= \sup\left(\varepsilon_{d0,t}, \overline{\varepsilon_{eq,t}}\right) \\ \overline{\varepsilon_{eq,t}} &= \max_{time}\left(\varepsilon_{eq,t}\right) \\ \varepsilon_{eq,t} &= \left|\boldsymbol{\varepsilon_{ELAS}} + \beta_{coupl}\, \boldsymbol{\varepsilon_{BC}}\right|_t \end{aligned} \quad (7)$$

with $\varepsilon_{d0,t} = \frac{R_t}{E}$ the tensile strain damage threshold, $< X >_+ = \max(X, 0)$, $|X|_t$ a tensorial norm involving the first and second invariants of the

tensor **X** [14], β_{coupl} a coupling factor to account for the effects of creep on damage.

Given its local nature, three actions are considered to increase its objectivity, alleviate the mesh-dependency and allow accurate crack opening post-processing respectively [16]:

- The characteristic size of the finite elements h_{EF} is imposed so as to be equal to the assumed size of the FPZ with respect to the hypothesis of one macrocrack per FPZ.
- The Hillerborg's energy-based regularization is used to avoid mesh dependency. This leads to the following relation between the parameter B_t in eq. 7 and the fracture energy G_F:

$$B_t = \frac{2\,E\,h_{EF}\,R_t}{2\,E\,G_F - h_{EF}\,R_t^2} \tag{8}$$

- The crack opening is obtained by post-processing the strain and damage fields as shown in eq. 9:

$$w_{ck} = h_{EF} \cdot d \cdot \left(\left|\left|\boldsymbol{\varepsilon}_{\mathbf{ELAS}}\right|\right| + \left|\left|\boldsymbol{\varepsilon}_{\mathbf{BC}}\right|\right|\right) \tag{9}$$

with $\left|\left|\mathbf{X}\right|\right| = \max(X_1, X_2, X_3, 0)$, $X_{1\leq i\leq 3}$ the Eigen values of the tensor **X**.

One should note that the mechanical properties (Young's modulus, tensile strength, fracture energy, elastic and creep Poisson ratios, compressive strength), are all considered age-dependent and are directly linked to the hydration rate α according to the maturity method.

3 STATISTICAL SIZE EFFECT LAW

The previous mechanical model is not inclusive of any size effects. To achieve that goal, the tensile strength R_t, defining both the tensile strain damage threshold ($\varepsilon_{d0,t}$) and the softening shape parameter (B_t), is set to be volume-dependent in line with equation (1). Considering the work in [7], the weighing function Ψ writes:

$$\Psi(\overrightarrow{x_0}, \vec{x}) = e^{-\pi\left(\frac{|\vec{x}-\overrightarrow{x_0}|}{D_c}\right)^2} \left(\frac{\left|\left|\boldsymbol{\sigma}\right|\right|}{\max_{\Omega}\left(\left|\left|\boldsymbol{\sigma}\right|\right|\right)}\right)^m \tag{10}$$

$\max_{\Omega}\left(\left|\left|\sigma\right|\right|\right)$ being the maximal value of $\left|\left|\sigma\right|\right|$ over the domain of interest Ω.

In this work, and to prevent the non-local implementation of the law in eq. 10 within a damageable framework, a simplified version of the original SEL in [7] is used. It consists of considering the maximal value over time of the maximal quantity $\int_{\vec{x}\in\Omega} \Psi(\overrightarrow{x_0}, \vec{x})\, d\vec{x}$ using a viscoelastic framework. This leads to a scalar quantity denoted V_{eff}^{max} which writes:

$$V_{eff}^{max} = \max_{time}\left(\max_{\overrightarrow{x_0}\,\epsilon\,\Omega}\left(\int_{\vec{x}\in\Omega} \Psi(\overrightarrow{x_0}, \vec{x})\, d\vec{x}\right)\right) \tag{11}$$

This quantity is then injected into equation (1), which leads to the definition of the tensile strength R_t used for the damage model:

$$R_t(\Omega) = R_t = \left(\frac{V_{eff}^{max}}{V_{ref}}\right)^{-\frac{1}{m}} R_{t,ref}(V_{ref}) \tag{12}$$

As for the statistical size effect, lognormal random fields are generated using the Expansion Optimal Linear Estimation (EOLE) method [17] and limiting the Karhunen-Loève (KL) development in eq. 2 to the first terms. Such truncation can be achieved in a way to verify, for instance, an arbitrary relative error on the computed variance compared to the desired one of 10% (In [20], it is demonstrated that the first hundred terms are sufficient to reach such precision).

Those random fields are associated with the Young's modulus instead of the tensile strength to allow a random simulation of concrete behavior prior to strain localization and during the softening phase (one can note that R_t does not influence the elastic behavior prior to $\varepsilon_{d0,t}$). Eventually, one obtains a random field of the damage model's direct inputs $\varepsilon_{d0,t}$ and B_t.

Five spatial correlation functions are explored in this work (Table 1) with a metric fluctuation length of the Young's modulus property [18].

Table 1: Spatial isotropic correlation functions

Correlation type	$\rho_Z(l_{flu}, u = \lvert\vec{x} - \vec{y}\rvert)$
None	$\rho_0 = \begin{cases} 1; u = 0 \\ 0; u \neq 0 \end{cases}$
Linear	$\rho_{lin} = < 1 - \frac{u}{l_{flu}} >_+$
Exponential	$\rho_{exp} = \exp\left(-\frac{2\,u}{l_{flu}}\right)$
Gaussian	$\rho_{gau} = \exp\left(-\pi\left(\frac{u}{l_{flu}}\right)^2\right)$
Sinusoidal	$\rho_{sin} = \frac{\sin\left(\pi\frac{u}{l_{flu}}\right)}{\pi\frac{u}{l_{flu}}}$

4 SENSITIVITY ANALYSIS

4.1 Application overview

In order to explore the effects of the spatial correlation of concrete properties (namely the $\varepsilon_{d0,t}$ and B_t inputs) on its cracking behavior, a particular structural volume called the gusset (Fig. 1) of an experimental 1:3 scaled containment building is considered at early age [13]. During the hydration phase, this area undergoes (partially) restrained (thermal and endogenous) shrinkages due to the presence of a hardened base slab which strain rate evolution in time is considerably less. This contrast leads to the development of tensile strains in the gusset volume that, when important, induce critical cracking (Fig. 1h) that might jeopardize the structural tightness. These cracks are mainly vertical due to the important tangential restraining compared to the one in the vertical direction. As one can see, based on visual inspections in Fig. 1h, the length (mean value of 40 cm and a coefficient of variation of 50%) and the spacing values (mean value of 21° and a coefficient of variation of 100%) observed on site are random. Though such randomness is expected to be due to the concrete material's heterogeneousness, the way such scattering is disposed on site is not known.

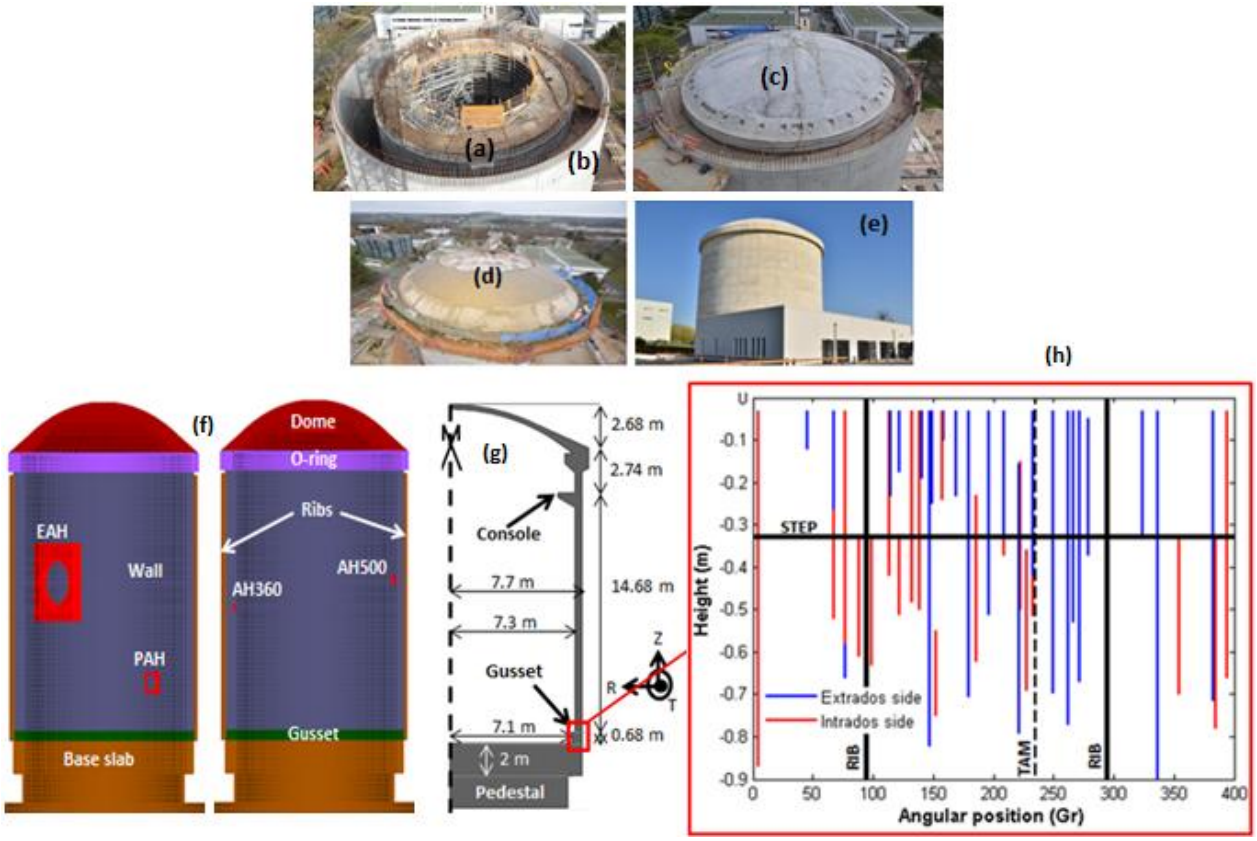

Figure 1: Experimental 1:3 scaled double walled containment building - VeRCoRs mock-up (a) inner wall (b) outer wall (c) inner dome (d) outer dome (e) full mock-up (f) schematic drawing of the inner wall structural parts(g) 2D-axis view of the VeRCoRs inner wall (h)in situ observations of the cracks' distribution at the gusset level from the intrados and extrados sides (12 days after casting).

So, an attempt to predict blindly the same cracking patterns using the previous stochastic model is undertaken hereafter relying only on several realizations of autocorrelated RF (Tab. 1) whereas all inputs are considered constant (no additional uncertainty other than the spatial variability is considered).

4.2 FE model

To reduce numerical cost and allow refined mesh for such large structure modeling, numerical calculations are performed at the scale of Representative Structural Volumes (RSV) shown in Fig. 2. Given the axisymmetric boundary conditions, only a portion of the gusset is modeled. To ensure physical objectivity and representativeness, this portion is estimated at the $1/24^{th}$ of the gusset circumference (which represents twice the considered fluctuation length of the Young's modulus). Also, so as to reproduce as accurately as possible the restraining effects, the model includes both the gusset (fresh lift) and the base slab (older hardened lift) with a realistic representation of steel rebars and prestressing cables sheaths (using 1D FE segments).

In terms of thermal boundary conditions (BC), Neumann-type BC are applied on the intrados and extrados sides of the gusset accounting for the effect of applied formwork. Used temperature profiles are issued from measurements on site. As for the mechanical BC, axisymmetric ones are applied on the lateral edges throughout the analysis (assuming that axisymmetry is hardly affected by the developed cracks at the RSV scale). Until the casting of the lift following the gusset, the upper surface is not restrained in any way and, for practical reasons and given its feeble structural rigidity, the formwork mechanical effect on concrete's behavior is overlooked. One should note that the steel elements are only active during the mechanical calculations using a perfect steel-concrete bond. Tab. 2 sums up relevant inputs for the numerical study. The full list of inputs is available in [9].

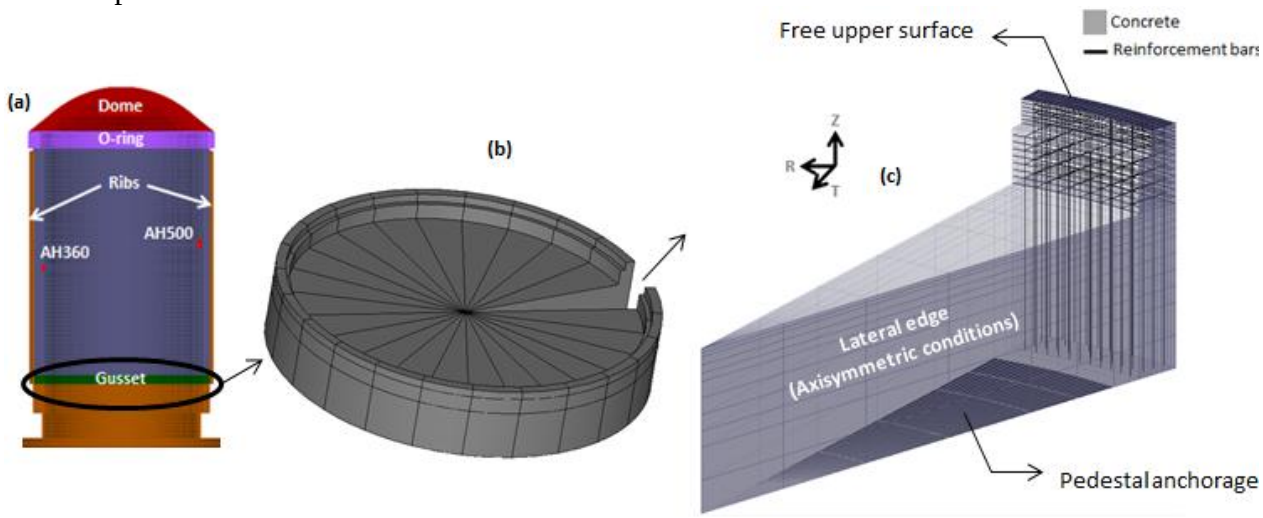

Figure 2: Modeling of a 1:3 scaled gusset structural volume at the RSV scale (a) 1:3 scale inner wall mock-up (b) gusset Structural Volume (SV) (c) gusset's Representative Structural Volume (RSV)

4.3 Numerical results vs. in situ observations

The effect of spatial correlation on the computed cracking response is explored via 30 realizations of RF for each function in Tab.1. For objective comparative analysis, the uncorrelated field realizations are kept the same for all functions (a preview of the obtained spatial scattering is depicted in Fig. 3).

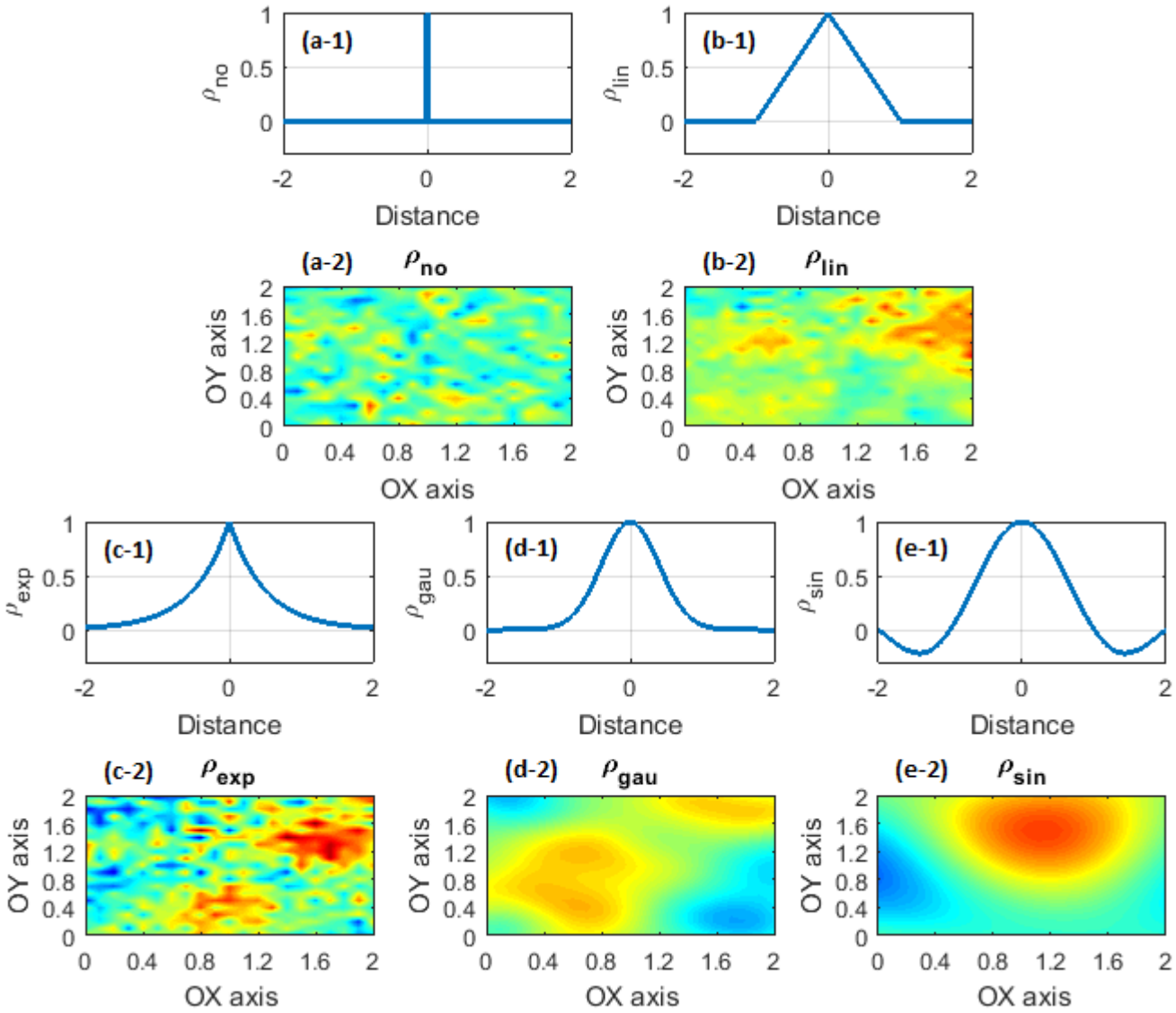

Figure 3: Spatial correlation effect on the distribution of a given lognormal random quantity (values scattered around 1 with a CV of 10% and a fluctuation length of 1 m): (a-1or2) No correlation (b-1or2) Linear correlation (c-1or2) Exponential correlation (d-1or2) Gaussian correlation (e-1or2) Sinusoidal correlation (a or b or c or d or e – 1) 1D correlation function (a or b or c or d or e – 2) 2D spatially correlated RF

For all configurations, three cracking patterns are obtained (Fig. 4b):

- **One** with two cracks developed in the vicinity of boundaries. The same pattern is obtained when no RF is used. This suggests that the introduced spatial variability, for those realizations, was not enough to overcome the deterministic one due to steel reinforcement discontinuities in the concrete volume. Indeed, steel elements can be seen as a source of a geometry-dependent ‘’deterministic’’ heterogeneity.
- **Two others** with one and two centered cracks respectively. For those realizations, the spatial scattering shows more effect than the deterministic heterogeneity which leads to random localization and propagation of cracks in the volume (not necessarily nearby the edges).

Eventually, the cracking of concrete is showed to be influenced by both: the introduced heterogeneity by RFs and the deterministic one due to the existence of steel elements in the 3D volume. Depending on the

generated realization and the distribution of weak points represented by the strain damage threshold $\varepsilon_{d0,t}$, one effect might be, statistically, more influential than the other.

Table 2: List of Thermo-Mechanical inputs (from [20])

Property	Value	Unit
λ_c	1.87	J/(s m °C)
ρ_c	2386	kg/m^3
C_c^p	880	J/(kg °C)
Q_∞	8.5 10^7	J/m^3
E_a^{th}	26 10^3	J/mol
α_{TH}	10	µm/(m °C)
α_{ES}	74	µm/m
R_t	2.9	MPa
E	36	GPa
G_F	77	N/m
h_{EF}	6-7	cm
$R_{t,ref}$	4.5	MPa
β_{coupl}	40	%
$(V_{ref})^{1/3}$	6.7	cm
$(V_{eff}^{max})^{1/3}$	34	cm
m	12	-
σ_E/μ_E	10	%
l_{flu}	1	m
D_c	1	m

In terms of the physical representativeness of the numerical results, three criteria are considered:

- Number of cracks per RSV: Using 30 RF realizations, the simulated number of cracks per RSV varies from 1 to 2 for, both, the upper (40 cm thick) and lower (60 cm thick) parts of the gusset. On site, and given a spacing value of 15°, the number of cracks varies from 0 to 3. So, the simulated patterns are realistic and, based on in situ observations, represent more than 50% of the observed patterns on site. The remaining 50% are associated with 0 and 3 cracks per 15° spacing. One might suspect the 30 realizations not to be enough to explore all cracking patterns observed on site. In addition, one is reminded that the model includes only the spatial variability of the Young's modulus (affecting the $\varepsilon_{d0,t}$ and B_t parameters) whereas, in reality, other properties remain spatially scattered (parameters in Tab. 2) and, ideally, their variability needs to be included in the model as well (especially the thermal and endogenous shrinkage coefficients in addition to the Young's modulus and tensile strength which have been demonstrated to be highly influential in [20]). However, the increase of the number of realizations (Monte Carlo Method) or the increase of the number of random parameters would lead to unreasonably high computational cost (given that each simulation lasts about 15 hours).
- Length of cracks per RSV: Using 30 RF realizations, the simulated cracks' lengths are systematically equal to the whole height of the gusset. On site, visual inspection shows variable lengths with cracks limited to the upper or lower parts of the gusset. with that regard, the improvement of model simulations requires (a) a more refined modeling of concrete heterogeneity using a smaller FE spatial discretization so as not to downgrade the quality of the discretized RF at its projection (b) improve the steel-concrete bond law to account for a non-null slip and allow some additional energy dissipation during stress transfer at cracking.
- Crack opening per RSV: The simulated crack opening values seem to be more dependent on the cracking pattern rather than the RF realization. In particular, and as expected for the same restraining effects, their openings decrease (not forcibly linearly) with the number of cracks (from ~60 µm for 1 centered crack, ~50 µm for two centered cracks to ~40 µm for two cracks at the boundaries). Unfortunately, on site measuring of early age cracks was achieved with a poor precision of 100 µm. So, all that can be concluded is that the simulated openings are in line with such observations since they are inferior than 100 µm.

4.4 Discussion related to the use of RFs

Based on 30 realizations of the defined Random Field, and as shown in Fig. 4a, the frequencies of each cracking pattern are strongly dependent on the retained spatial

correlation. In particular, the following observations are made:

- In the absence of spatial correlation (Fig. 3a), and given the independence of values in space, the simulated statistical size effect is maximal. This is observed though the obtained cracking patterns (Fig. 4a-ρ_0) where the deterministic-like response (cracks on boundaries) was obtained less than 10% of the times whereas more than 90% correspond to centered ones.
- When using spatial correlation (Fig. 3b-e), and depending on the used autocorrelation function ρ, the frequencies of each cracking pattern vary. For the sinusoidal function (Fig. 4a-ρ_{sin}), the frequency of the cracking pattern with cracks at boundaries is high (more than 50%) which leads to the assumption that the effect of the introduced variability using RFs hardly overcomes the effect of the ‘’deterministic’’ heterogeneity. So, for the same fluctuation length, the efficiency of the sinusoidal autocorrelation function in terms of statistical size effect modeling is limited compared to the other functions. The efficiency of RFs (in terms of having cracks not forcibly nearby boundaries) tends to increase as the linear (Fig. 4a-ρ_{lin}), Gaussian (Fig. 4a-ρ_{gau}) and exponential (Fig. 4a-ρ_{exp}) autocorrelations are used respectively.

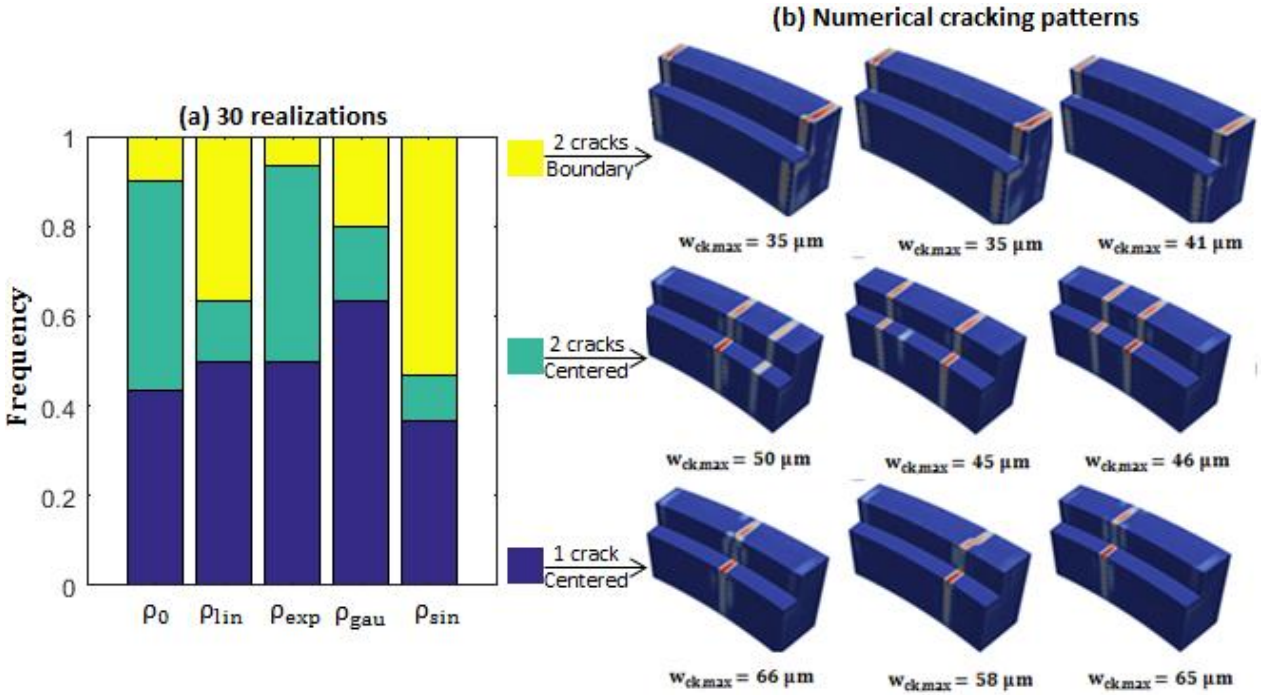

Figure 4: Dependence of the statistical distribution of the cracking patterns on the spatial correlation (a) frequency variation with the auto correlation functions (b) cracking patterns at 12 days after casting

It is then interesting to see that the results obtained using exponential correlation (Fig. 4a-ρ_{exp}) show the least frequency of cracks nearby boundaries and maximize the statistical effect on the simulated cracking patterns. It is worth mentioning that the same exponential function has been suggested in the conclusions of the EvaDéOS project [19]. However, this recommendation was only based on in situ observations and not to aim at a maximization of concrete’s statistical size effects. In all cases, given the important effect of spatial correlation on the resultant cracking patterns’ frequencies, it seems mandatory to perform spatial correlation measuring on site or at intermediate structural scales in order to accurately assess the cracking risk and quantify the frequencies of each cracking pattern

- In this analysis, only spatial correlation

effect (in terms of the strain damage threshold and softening behavior) on the resultant cracking patterns has been explored. However, one should note that uncertainties also concern other parameters of thermal (hydration heat, thermal capacity, etc.), chemical (hydration kinetic, activation energy, etc.) and mechanical (endogenous and thermal coefficients, fracture energy, etc.) nature. The variability of those inputs is expected to have an effect on the cracking response and cannot be, a priori, neglected. With that regard a full sensitivity analysis is required to compare the effect of each input's variability on the model's response and select only the most influential. Though such work is achievable, one should keep in mind that it requires hefty computational cost and wonder if other methods could be used (more efficient and less cost consuming); particularly through the use of Surface Response Methods [20]

5 CONCLUSIONS

In this contribution, the sensitivity of the structural cracking response to the spatial correlation of concrete damage properties has been performed. Using a local and energy-regularized damage model within a thermo-mechanical framework at early age, and based on the considered example of a RSV from a 1:3 nuclear containment building, the following conclusions are retained:

- The spatial correlation of concrete's damage properties mainly affects the frequencies of the cracking patterns which remain the same regardless of the applied auto correlation function.
- The absence of spatial correlation maximizes the effect of statistical size effect on concrete cracking. Such effect is reduced when using an exponential, Gaussian, linear or sinusoidal function respectively (considering the same fluctuation length).
- The efficiency of RF to describe various cracking patterns of concrete remains questionable in terms of computational cost and adequacy with Monte Carlo Methods. Alternative methods need to be considered to enhance such methodological aspects, for example based on Surface Response Methods.
- The spatial correlation strongly affects the distribution of the cracking patterns of concrete. Therefore, the identification and measurement of such randomness needs to be achieved systematically to perform reliable predictive simulations of concrete cracking at the structural scale.

6 ACKNOWLEDGEMENT

This work was supported by EDF-SEPTEN/DTG/CIH within the Chair PERENITI agreement with the Grenoble INP Partnership Foundation and by the joint MACENA and ENDE project fund (ProjetIA-11-RSNR-0009 and ProjetIA-11-RSNR-0012).

REFERENCES

[1] Giry C., Dufour F., Mazars J. 2011. Stress-based nonlocal damage model. *Solids and Structures*, **48**(25-26).

[2] Bažant Z. P., 1999. Size effect on structural strength: a review. *Archive of Applied Mechanics*. **69**:703-725

[3] Weibull W., 1939. A statistical theory of the strength of materials. *Royal Swedish Academy of Engineering Science*. **151**:1-45.

[4] Hild F. 1994. Volume and Stress Heterogeneity Effects in Ceramics and Fiber-Reinforced Ceramics. *Probabilities and Materials*. **269**: 42-438.

[5] Hillerborg A., Modeer M., Petersson P.-E., 1976. Analysis of crack formation and crack growth in concrete by means of fracture mechanics and finite elements. *Cement and Concrete Research*. **6**:773-781.

[6] Mazars J., 1984. Application of Continuous Damage Mechanic to Non-Linear Behavior of Concrete Structures. *Open Journal of Civil Engineering*. **5**.

[7] Sellier A., Millard A., 2014. Weakest link

and localisation WL2: a method to conciliate probabilistic and energetic scale effects in numerical models. European Journal of Civil Engineering. **18**:1177-1191.

[8] Rossi P., Wu X., 1992. Probabilistic model for material behaviour analysis and appraisement of concrete structures. *Magazine of Concrete Research*. **44**:27-280

[9] Bouhjiti D. E.-M., Baroth J., Briffaut M., Dufour F., Masson B., 2018. Statistical modeling of cracking in large concrete structures under Thermo-Hydro-Mechanical loads: Application to Nuclear Containment Buildings. Part 1: Random field effects (Reference analysis). *Nuclear Engineering and Design*. **333**:196-223.

[10] Ghanem R., Spanos P., 1991. Stochastic finite elements – A spectral approach. *Revised ed. Dover Pub. NY. USA*. 17-41.

[11] Vanmarcke E., 1983. Random field: analysis and synthesis. *The MIT Press. Cambridge. Massachusetts*.

[12] Vořechovský M., 2007. Interplay of size effects in concrete specimens under tension studied via computational stochastic fracture mechanics. Solids and Structures. **44**:2715-2731.

[13] VeRCoRs project: xing-events.com/OLD-EDF-vercors-project.html

[14] Mazars, J., Hamon, F., Grange, S., 2015. A new 3D damage model for concrete under monotonic, cyclic and dynamic loadings. *Materials and Structures*. **48**: 3779-3793

[15] Fichant S., La Borderie C., Pijaudier-Cabot G., 1999. Isotropic anisotropic description of damage in concrete structures. *Mechanics of Cohesive-Frictional Materials*. **4**: 399- 359.

[16] Bouhjiti D. E.-M., El Dandachy E. M., Dufour F., Dal Pont S., Briffaut M., Baroth J., Masson B., 2018. New continuous strain-based description of concrete's damage-permeability coupling. *Numerical and Analytical Methods in Geomechanics*. 1-27.

[17] Li C., Der Kiureghian A., Ke J. B., 1993. Optimal discretization of random fields. *Engineering Mechanis*. **119**: 1136-1154

[18] de Larrard, T., Colliat J. B., Benboudjema F., Torrenti J. M., Nahas G., 2010. Effect of the young modulus variability on the mechanical behaviour of a nuclear containment vessel. *Nuclear Engineering and Design*. **240**:4051–4060.

[19] EvaDéOS project: https://agence-nationale-recherche.fr/en/anr-funded-project/?tx_lwmsuivibilan_pi2[CODE]=ANR-11-VILD-0002

[20] Bouhjiti D. E.-M., 2018. Probabilistic analysis of cracking and tightness of reinforced and prestressed large concrete structures. *PhD thesis [in French]*. Univ. Grenoble Alpes, France.